Development of novel UV emitting single crystalline film scintillators

2011 J. Phys.: Conf. Ser. 289 012029

(http://iopscience.iop.org/1742-6596/289/1/012029)

Development of novel UV emitting single crystalline film scintillators

Yu Zorenko[1], V Gorbenko[1], V Savchyn[1], T Voznyak[1], M Nikl[2], J A Mares[2],T Martin[3], P –A Douissard[3]

[1] Laboratory of Opoelectronic Materials (LOM), Electronics Department of Ivan Franko National University of Lviv, 79017 Lviv, Ukraine
[2]Institute of Physics of ASCR, 162 53 Prague, Czech Republik
[3]ESRF, Instrument Support Group, 6 rue Jules Horoeitz, 38043 Grenoble, France

E-mail: zorenko@electronics.wups.lviv.ua

Abstract. The work is dedicated to development of new types of UV –emitting scintillators based on single crystalline films (*SCF*) of aluminimum perovskites and garnets grown by the liquid phase epitaxy (LPE) method. The development of the following three types of UV *SCF* scintillators is considered in this work: i) Ce-doped *SCF* of Y-Lu-Al-perovskites with Ce^{3+} emission in the 360-370 nm range with a decay time of 16-17 ns; ii) Pr-doped *SCF* of Y-Lu-Al garnets with Pr^{3+} emission in the 300-400 nm range with a decay time of 13-17 ns; iii) La^{3+} and Sc^{3+} doped *SCF* of Y-Lu-Al-garnets, emitting in the 290-400 nm range due to formation of the $La_{Y,Lu}$, $Sc_{Y,Lu}$ and Sc_{Al} centers with decay time of 250-575 ns. The results of testing the several novel UV-emitting *SCFs* scintillators for visualization of X-ray images at ESFR are presented. It is shown that the UV emission of the LuAG:Sc, LuAG:La and LuAG:Pr *SCFs* is efficient enough for conversion of X-ray to the UV light and that these scintillators can be used for improvement of the resolution of imaging detectors in synchrotron radiation applications.

1. Introduction

During the last 30 years the liquid phase epitaxy (LPE) shows oneself as a beneficial method for the development of new types of luminescent materials based on *single crystalline films (SCF)* of oxide compounds (garnets, perovskites, sapphire, silicates, tungstates)[1-3]. The fields of application of such *SCF* are now extended to α- and β- scintillators, screens for visualization of X-ray images, cathodoluminescent screens as light sources for scanning optical microscopes, laser media and luminescent converters of LED radiation [1-9].

In several previous works [2,4,10,11] we have demonstrated the creation by LPE method of the *SCF* scintillators based on $Y_3Al_5O_{12}$:Ce (YAG:Ce) and $Lu_3Al_5O_{12}$ (LuAG:Ce) garnets emitting in visible (450-750 nm) range with a decay time of 70 and 50 ns respectively. We have also shown [12-16] that these *SCF* scintillators in comparison with bulk *single crystal (SC)* analogues are characterized by faster Ce^{3+} emission decay under high energy excitation, substantially less (by 4.5-8 times) content of slow emission components and higher energy resolution due to the absence in them of Y_{Al} and Lu_{Al} *antisite defects (ADs)* and low concentration of vacancies as luminescence and trapping centers.

In this work, we focus on the development of emitting in the UV range *SCF* scintillators based on garnet and perovskites compounds. The reasons for the development of such scintillators are as follows:

1.Shift of the emission spectra of *SCF* scintillators into the UV range with respect to recently developed *SCFs* of LuAG:Ce anf YAG:Ce garnets, emitting in visible range, in principle can result in the faster emission decay, larger light yield (LY) and higher energy resolution [4,15]. Specifically, we plan to extend the class of novel SCF scintillators which effectively emit in UV ranges, on Ce-doped perovskites (YAP:Ce and LuAP:Ce) and Pr^{3+}-doped garnets (LuAG:Pr and YAG:Pr).

2. Microimaging techniques with synchrotron or X-ray radiation for applications in microtomography and industry [5-7] demands fast, on-lne X-ray image detectors with spatial resolution in the μm or sub-μm range. For this task, a X-ray image detectors based on YAG:Ce SCF, microscope optics, a low-noise CCD camera, operated at X-ray energies of 10-50keV have been recently developed [5,6]. The spatial resolution of X-ray images of 0.8 μm FWHM is achieved . Future increase of the spatial resolution of detector requires creation of the *SCF* scintillating screens emitting the UV light. Registration in the UV range could increase the spatial resolution of a detector according to the formula:$0.61*\lambda/NA$, where λ is the emission wavelength, NA is the numerical aperture of the optics.

In this work we have studied the scintillation properties of several types of UV emitting *SCF* scintillators prepared by LPE method. For visualization of X-ray images in the UV light we also tested at ESRF[3] the novel *SCF* scintillators based on LuAG garnet and LuAP perovskites compounds which have significantly higher density (ρ=6.67 and 8.34 g/cm^3) and effective atomic number (Z_{eff}=59 and 62) [6,7,10,11] as compared to commonly used YAG (ρ=4.6 g/cm^3, Z_{eff}=29) [4,5]. As mentioned above, for creation of the intense UV light, the Pr^{3+} as well as La3+ and Sc^{3+} ions can be used as activators in LuAG *SCF* and Ce^{3+} ions in LuAP *SCF* respectively.

2. Growth of *SCF* scintillators and experimental technique

The series of Pr, La and Sc-doped YAG and LuAG and Ce-doped YAP and LuAP *SCF* scintillators were grown in LOM Lviv University by the LPE methods onto YAG and YAP substrates, respectively, with super-cooled melt – solution (MS) based on the PbO-B_2O_3 flux at relatively low temperatures (950-1100 °C) as compared to Czochralski – grown *SC* (~2000°C). The thickness of the *SCF* scintillators was varied in the 4.8-45 μm range. It is important to note, that we did not use any additional doping to reduce the significant differences in the lattice constants of the LuAG- and LuAP- based SCF and the YAG and YAP substrates which are equal to about 1.0 and 1.4% respectively [18-20].

The lower growth temperature of *SCF* results in absence of Y_{AL} and Lu_{AL} *ADs* and decrease of concentration of other type of defects in *SCF* in comparison with bulk *SC* analogues [13,17]. On the other hand, flux components can be introduced in the *SCF* that might have detrimental influence on their emission and scintillation properties [21-24]. Usually, the *SCFs* prepared from the PbO –based flux, can contain lead ions preferably in the Pb^{2+} charge state. Since the PbO – based melt dissolves the Pt-crucible, Pt^{4+} ions can also be introduced in the garnet or perovskites lattices. As a consequence, various locally non- compensated lattice defects can be created, which may result in the decrease of the scintillation efficiency and light yield of *SCF* scintillators (LY) [2,4,20,24].

Therefore, the LY of Pr-, La- and Sc-doped YAG and LuAG *SCF* and Ce-doped YAP and LuAP *SCF* scintillators in the UV range can strongly depend on the concentration in them of activators as well as Pb^{2+} and Pt^{4+} dopants. In principle, the suitable LY of the mentioned *SCF* can be achieved by means of optimization of the activator content in MS [2,10,21,22,24]. Specifically, due to significant difference in the segregation coefficient of La^{3+}, Sc^{3+} and Pr^{3+} ions at the crystallization of YAG and LuAG *SCF* onto YAG substrates [20,21] and Ce^{3+} ions at crystallization of YAP and LuAP *SCF* onto YAP substrates [20,24], the concentrations of Sc_2O_3, La_2O_3, Pr_2O_3 and CeO_2 activated oxides in MS was varied in the 4.6-6.7,1-8.2, 3.1-8.6 and 2-20 mole % ranges, respectively. At the same time, the concentration of different impurities in the *SCF* depends not only on the content of activated oxides in MS, but is also strongly influenced by the *SCF* growth temperature. Of the most importance is that the concentrations of dopants as well as Pb^{2+} and Pt^{4+} flux impurities increase with decreasing the growth temperature and vice versa [21,22,24]. For these reasons we have used relatively high growth temperatures above 950°C for *SCF* preparation.

The content of different dopants in *SCF* was determined using JEOL JXA-8612 MX electron microscope and presented in table 1 for different series of *SCF* scintillators.

Table1. Relative LY of the best samples in series of UV-emitting SCF scintillators in comparison with standard bulk *SC* analogues under excitation by α-particles of Pu^{239} sources (5.15MeV). The concentration of Y_{Al} and Lu_{Al} *ADs* estimated by XRD analysis is presented for undoped YAG and LuAG *SC*

Dopant	Scintillators	Activator content, at. %	Maximum of emission band, nm	Decay time of main emission component, ns	LY, % Am^{241}(3 μs)/ Pu^{239}(0.5 μs)
Ce	YAP:Ce *SCF* (PbO flux)	0.08	366	13.1	36.1/25.5
	YAP:Ce *SCF* (BaO flux)	0.053	373	16.1	- /23.8
	$Y_{0.4}Lu_{0.6}$AP:Ce *SCF* (PbO flux)	~0.04	363	16.0	- /10.2
	LuAP:Ce *SCF* (PbO flux)	0.013	358	16.9	- /7.65
	YAP:Ce *SC*	~0.1	366	16.2	100/100
	$Lu_{0.3}Y_{0.7}$AG:Ce *SC*	~0.1	375	17.1	83.2/56.3
Pr	YAG:Pr *SCF*	0.085	323	13	33.7/21.6
	LuAG:Pr *SCF*	0.66	305	17	29.8/24.9
	YAG:Pr *SC*	0.19	327	17.6	75.4/60.8
	LuAG:Pr *SC*	0.31	308	18.6	59.3/55.6
La	YAG:La *SCF*	0.045	297		13.6/6.9
	$Lu_{2.74}Y_{0.25}Al_5O_{12}$:La *SCF*	0.04	282	170	15.9/11.0
	YAG:La *SC*	0.085	298	575	- /21.0
	undoped YAG *SC*	0.19*	292; 332	350; 1490	19.8/10.9
	undoped LuAG *SC*	0.575*	296; 334	440, 3020	- /18.8
Sc	$Y_{2.96}Sc_{0.475}Al_{4.555}O_{12}$ *SCF*	2.38	322	~750	38.7/26.7
	$Y_{2.84}Lu_{0.14}Sc_{0.37}Al_{4.65}O_{12}$ *SCF*	1.85	314	~650	57.4/48.2
	$Y_{2.76}Lu_{0.18}Sc_{0.715}Ga_{0.095}Al_{4.25}O_{12}$ *SCF*	3.60	330	~800	28.0/17.8
	$Lu_{2.67}Sc_{0.585}Al_{4.745}O_{12}$ *SCF*	2.93	312	245; 390	27.6/21.8
	$Y_{2.995}Sc_{0.077}Al_{4.864}O_{12}$ *SC*	0.39	314	~580	69.3/45.9
	$Lu_{2.773}Sc_{0.022}Al_{5.205}O_{12}$ *SC*	0.11	290	1330	31.4/21.8

For estimation of the scintillation efficiency in the UV range of the developed *SCF* scintillators with garnet and perovskites structure the relative LY measurements of all corresponding series *SCF* samples were performed in comparison with standard samples of YAG:Pr, LuAG:Pr, YAG:La, YAG:Sc, LuAG:Sc,YAP:Ce and $Lu_{0.3}Y_{0.7}$AG:Ce bulk *SC* scintillators under excitation by α-particles of Pu^{239} (5.15 MeV) and Am^{241} (5.4857 MeV) sources with a penetration length in studied materials of about 10-12 μm. For LY measurements we used the detectors based on FEU-110 and hybrid DEP PPO 475B PMT types which have the maximum sensitivity in the 250-375 and 200-400 nm ranges and mulitichannel single – photon counting system working within a time interval of 0.5 and 3 μs, respectively. The results of YL measurements are presented in Table 1.

For the correct characterization of the luminescent properties of the tested series of UV-emitting *SCF* we used measurements of their cathodoluminescence (CL) spectra under pulsed e-beam excitation (a pulse duration of 2 μs and a frequency of 30-3 Hz) with energy of electrons of 9keV and a beam current of 100 μA. Emission spectra were corrected for the spectral dependence of the detection part consisting of DMR-4 monochromator and FEU-106 photomultiplier (PMT).

The decay kinetics of luminescence were measured at 300K in the time interval 0-200 ns under excitation *SCF* and *SC* scintillators by synchrotron radiation (SR) with a pulse duration of 0.126 ns at Superlumi experimental station in HASYLAB,DESY.

3. Luminescence spectra and LY of *SCF* scintillators

3.1 Ce-doped perovskites

The CL spectra of YAP:Ce and LuAP:Ce SCF (Fig.1, curve 1 and 2) present intensive emission band in the UV (320-450 nm) range related to the $5d^1 \rightarrow 4f(^2F_{5/2,7/2})$ transitions of Ce^{3+} ions [19,20,24]. It is important to note that the short-wavelength part of the Ce^{3+} emission spectra in YAP:Ce and LuAP:Ce *SCF*, growth from PbO – based flux, can be strongly distorted by the UV emission band of Pb^{2+} ions peaked at 340 nm [25] (Fig.1). This caused a notable short-wavelength shift of the emission spectrum of YAP:Ce *SCF*, grown from the PbO-based flux, with respect to the luminescence spectrum of the same *SCF*, grown from the lead-free flux. Other low-intensity complex emission band in YAP:C and LuAP:Ce *SCF*, related to the luminescence of excitons localized around of Pb^{2+} ions, is located in the visible range with maximum approximately at 590 nm (Fig.1).

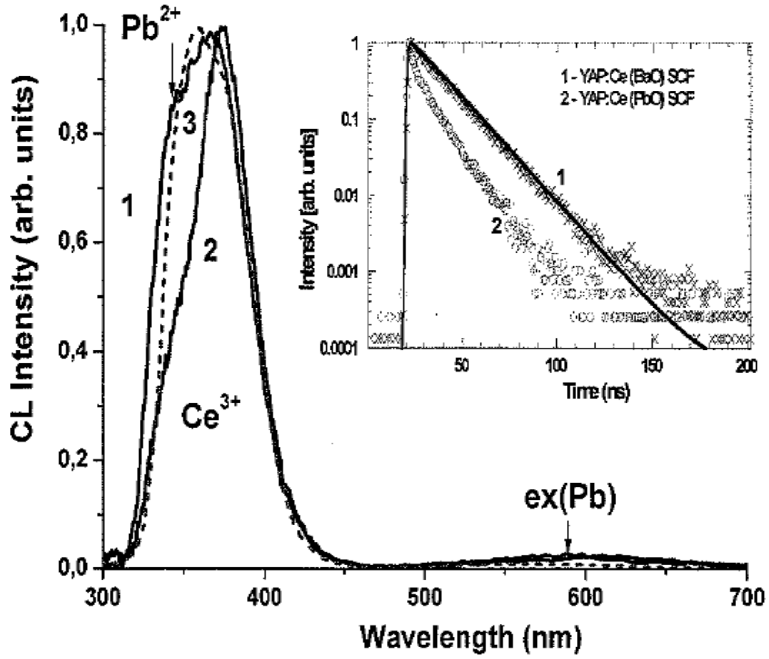

Figure 1. Normalized CL spectra of YAP:Ce (1,2) and LuAP:Ce (3) *SCF*; insert – normalized luminescence decay kinetics of YAP:Ce *SCF*, grown from the BaO- (1) and PbO-based (2) flux under excitation in Ce^{3+} absorption band at 300 nm; T=300K

As can be seen from Table 1, the LY of YAP:Ce and especially of LuAP:Ce *SCF* scintillators , grown even at the optimal CeO_2 content in the MS of 10-20 mol%, is significantly lower (by 3.9 anf 7.6 times, respectively) then that of their YAP:Ce and (Y-Lu)AP:Ce *SC* analogues. The main reason for such low LY of YAP:Ce and LuAP:Ce *SCF* scintillators is the large incorporation of Pb^{2+} ions in *SCF* of perovskites in comparison with SCF of garnets [23] due to larger volume of cub-octahedral position in perovskites lattice with respect to the dodecahedral position of garnet lattice, where Pb^{2+} ions are localized. We also note that the LY of (Y-Lu)AP:Ce *SCF* systematically decrease with increasing the Lu content up to a value of 7.65% for LuAP:Ce *SCF* as compared to that of YAP:Ce *SC*. This effect can be explained by the large incorporation of Pb^{2+} ions in LuAP-based *SCF* with respect to YAP *SCF* due to preferable Lu-Pb pair incorporation in comparison with Y-Pb pair in the case of *SCF* crystallization of both types of perovskites onto YAP substrates [20].

We have also observed the visible acceleration of decay kinetics of the Ce^{3+} luminescence in YAP:Ce *SCF*, grown from PbO-based flux (Fig.1, insert, curve 2). The decay curve for this YAP:Ce *SCF* is strongly non-exponential and can be quantitatively characterized by an average decay time of 13.1 ns

(Table 1). Such acceleration of the decay kinetics of the Ce^{3+} luminescence in YAP:Ce *SCF* scintillators grown from PbO-based flux, can be caused by the energy transfer from Ce^{3+} ions to Pb^{2+} related centers, which have the excitation bands in the 350-370 nm range, well overlapped with Ce^{3+} emission band [26]. In opposite to this *SCF*, the decay kinetics of the Ce^{3+} luminescence in YAP:Ce *SCF*, grown from BaO – based flux, is strongly exponential (insert of Fig.1, curve 2) with a decay time of 16 ns, which is very close to the decay time of the Ce^{3+} emission in YAP:Ce *SC* (Table 1).

From calculation of the integral of normalized decay curves for YAP:Ce *SCF*, grown from the BaO- and PbO-based fluxes, which is equal to 100 and 46%, respectively, we can conclude that in the last *SCF* scintillators the losses of more than 50% excitation energy take place due to energy transfer away from Ce^{3+} $5d^1$ excited state to Pb^{2+} - based centers [24]. Such huge loss can partly explain such low LY of YAP:Ce and LuAG:Ce *SCF* scintillators, grown from PbO – based flux (Table 1).

3.2 Pr^{3+} doped garnets

The CL spectra of YAG:Pr and LuAG:Pr show intensive and fast emission in the 290-450 nm range with main maxima at 305 and 322 nm, respectively, caused by the $5d^14f^1 \rightarrow 4f^2(^3H_4, ^3H_5, ^3H_6, ^3F_{3(4)})$ transition of Pr^{3+} ions. The sharp-line emission bands peaked at 487, 501 and 563 nm as 609-620, 638 and 663 nm in the visible range, are related to the transition from the $^3P_0$ and $^1D_2$ levels of the $4f^2$ shell to the $^3H_{6,5,4}$ levels of the ground state of Pr^{3+} ions (Fig.2,curve 2). The content of slow visible emission is significantly lower in LuAG:Pr *SCF* than in YAG:Pr *SCF* (Fig.2).

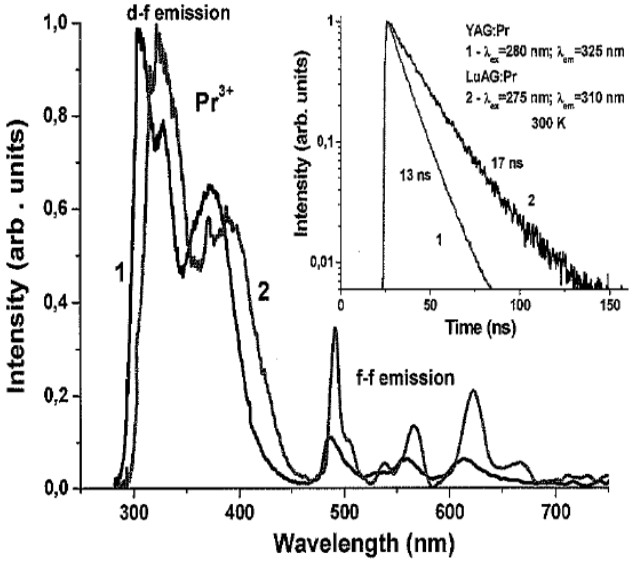

Figure 2. CL spectra and decay kinetics (insert) of Pr^{3+} luminescence in YAG:Pr (1) and LuAG:Ce (2) *SCF* at 300K

As can be seen from Table 1, the LY of YAG: Pr and LuAG:Pr *SCF* scintillators is significantly lower (by 2.2-2.8 times) then that of their *SC* analogues. This result contradicts with the results of our previous investigations of the LY of Ce-doped YAG and LuAG SCF scintillatores, emitting in the visible (515-530 nm) range, with their SC analogues [13].Specifically, for these compounds the comparable LY of *SCF* and *SC* scintillators occurs [13]. Taking into account the absence of Y_{Al} and Lu_{Al} *AD* and low concentration of vacancy – type defects in YAG and LuAG *SCF* [13,14], the main reason for lower LY of the Pr^{3+} - doped *SCF* scintillatores in comparison with *SC* of these oxides is the strong quenching influence of Pb^{2+} flux related impurity. Thus, based on the results presented in Table 1, we can conclude that significantly larger influence of Pb^{2+} flux dopant on the UV luminescence of Pr^{3+} ions takes place in YAG:Pr and LuAG:Pr *SCF* in comparison with the influence of this dopant on the Ce^{3+} luminescence n the visible range in Ce-

doped *SCF* of these garnets [13,23]. The mechanism of $Pb^{2+} \rightarrow Pr^{3+}$ energy transfer is considered in detail in [26].

3.3 La doped garnets

The CL spectra of YAG:La SC, YAG:La and LuAG:La *SCF* are shown in Fig.3a. The intensive complex emission bands in the 250-450 nm range are caused by La^{3+} isoelectonic impurities. Namely, these bands in YAG:La and LuAG:La *SCF* presents superposition of two close-lying bands peaked at 298, 305 nm and 267,282 nm (Fig.3a,curves 2 and 3 respectively). The short-wavelength bands are related to the luminescence of exciton localized around $La_{La,Y}$ centers (La^{3+} ions in the dodecahedral sites of Y^{3+} or Lu^{3+} cations), when the long-wavelength bands are caused by the recombination luminescence of La_Y and La_{Lu} centers. In YAG:La and LuAG:La *SCFs*, grown from PbO-based flux, the long-wavelength wngs of complex UV emission bands, caused by La dopant, are also overlapped with the UV emission band of Pb2+ ions peaked at 350-360 nm [23] (Fig.3a, curve 2 and 3). It is worth to note that the nature of the emission centers formed by La^{3+} dopant in YAG and LuAG host is similar in the whole to the nature of the centers responsible for the relatively intensive intrinsic UV luminescence of YAG and LuAG bulk *SCs* (Fig.3 b, curves 1 and 2, respectively). Specifically, this band in YAG and LuAG *SCs* presents superposition of the luminescence of excitation localized around Y_{Al} and Lu_{Al} *ADs* (Y^{3+} and Lu^{3+} cations in the octahedral sites of Al^{3+} cations) in the band peaked at 292 and 296 nm and the recombination luminescence of Y_{Al} and Lu_{Al} *ADs* in the bands peaked at 332 and 334 nm, respectively [13].

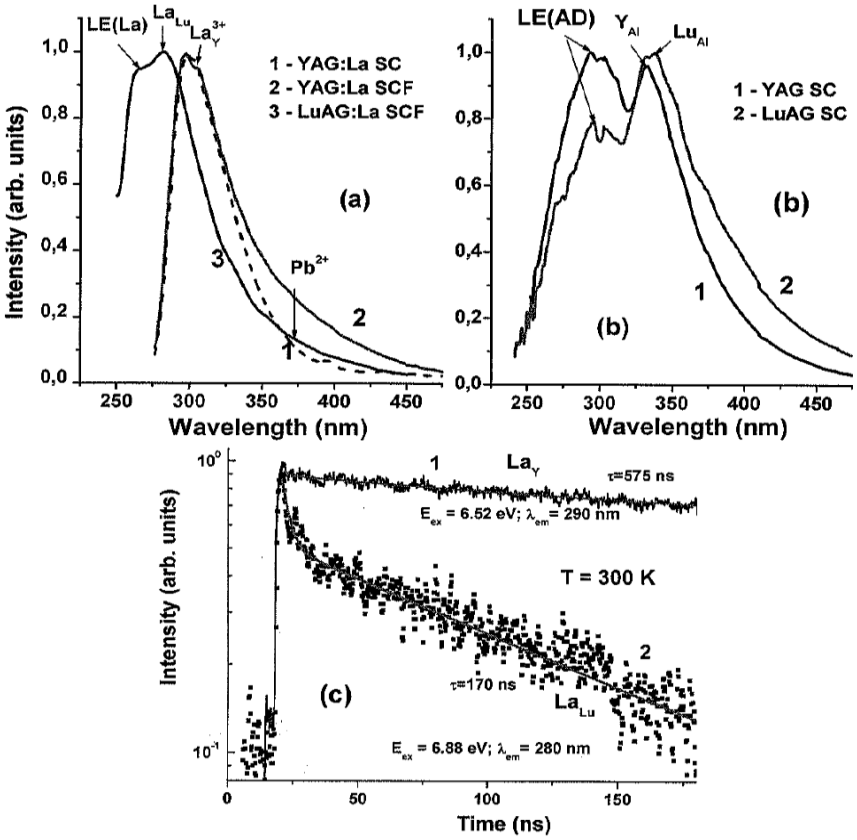

Figure 3.(a)-CL spectra of YAG:La *SC*(1), YAG:La *SCF*(2) and LuAG:La *SCF*(3) at 300K; (b)-CL spectra of undoped YAG (1) and LuAG (2) *SC* at 300K;(c)-decay kinetics of luminescence of La_Y (1) and La_{Lu} (2) centers at 290 and 285 nm in YAG:La and LuAG:La *SCF* at 300K under excitation by SR at 6.52 and 6.88 eV, respectively.

The decay kinetics of luminescence of La_Y and La_{Lu} centers in YAG:La and LuAG:La *SCF*, under excitation in the exciton range with an energy of 6.52 and 6.88 eV, respectively, is shown in Fig.3c. The decay times of main component of La_Y and La_{Lu} centers luminescence are 560 and 170 ns, respectively.

The LY of YAG:La and LuAG:La *SCF* and *SC* scintillators is not so much influenced by Pb^{2+} flux impurity but strongly depend on the La content in garnet host. As can be seen from Table 1, the LY of YAG:La and LuAG:La *SCF* scintillators with La content of 0.04-0.05 at.% is by 2-3 times lower in comparison with YAG:La (0.085at.%) *SC*. Also the LY of YAG:La and LuAG:La *SCF* is significantly (by 2-4 times) lower than that of Sc-doped YLuAG and LuAG SCF. Such a low LY of La-doped *SCF* is mainly caused by very low (0.005) segregation coefficient of La^{3+} ions at the crystallization of YAG:La and LuAG:La *SCF* in comparison with that (0.14) for YAG:La *SC* analogues [21]. As a result, the rather small (0.04-0.045 at.%) concentration of La^{3+} ions can be achieved in LPE-grown YAG:La and LuAG:La *SCF* (Table 1) even at large (above 8 mole %) content of La_2O_2 dopant in MS in comparison with an optimum value of 0.4-1.85 at.% for Sc-doped *SCF* analogues of these garnets.

3.4 Sc-doped garnets

In contrast to La^{3+} ions, Sc^{3+} isoelectronic impurity in YAG and LuAG host has relatively high (0.8-0.55 and 0.2-0.4, respectively) segregation coefficients [21,22]. This allows readily achieving the optimum values of Sc doping for both *SC* and *SCF* of these garnets in range 0.4 – 2.4 at.% at which the highest LY scintillators are observed (Table 1). The incorporation of Sc^{3+} ions in YAG and LuAG *SC* and *SCF* at total scandium content $x<0.3$ formula units (f.u) results in the Sc^{3+} ions localization both in the dodecahedral {c}- and octahedral (a)-sites in ratio of about 40:60% [27] with formation $Sc_{Y,Lu}$ and Sc_{Al} centers, respectively. At higher content the Sc^{3+} ions occupy predominantly the (a)-sites of garnet lattice (insert in Fig.4) [27]. At the same time, the relation between the $Sc_{Y,Lu}$ and Sc_{Al} centers in YAG and LuAG host can be changed by substitution of the {c}- and (a) – sites of garnet lattice by other co-dopants with smaller or larger dimensions. Specifically, due to partial substitution of $^{Y3+}$ cations by the Lu^{3+} ions, or Al^{3+} cations by the Ga^{3+} ions, the content of $Sc_{Y,Lu}$ center in $(YLu)_3Al_5O_{12}$ and $(YLu)_3Al_5GaO_{12}$ *SCF* can strongly decrease up to 7-8% (Table 1).

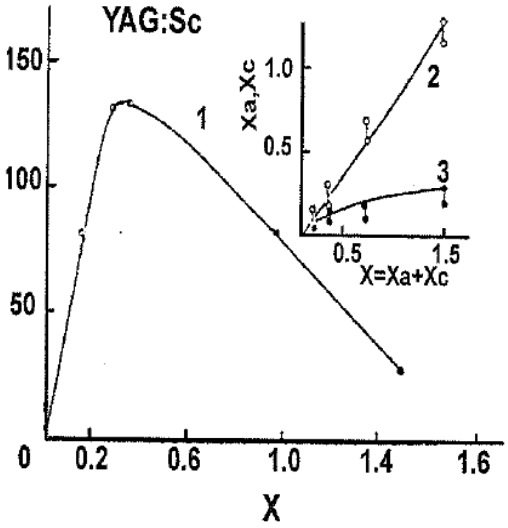

Figure 4. Dependence of integral intensity of CL (1) and concentration of Sc_{Al} (2) and Sc_Y (3) centers on total scandium content in YAG:Sc *SCF*.

Thus, in Sc-doped garnets the formation of two types of emission centers ($Sc_{Y,Lu}$ and Sc_{Al}) takes place which can contribute to the intensive UV luminescence of these compounds and compete in the processes of energy transfer [27,28]. Specifically, above mentioned distribution of Sc^{3+} ions over the {c}- and (a) – sites explains the complex dependence of the positions of the maximum emission bands of YAG:Sc and LuAG:Sc *SCF* on the Sc content (Fig.4). At relatively small (x=0.05-0.15 f.u.) Sc concentration, the

emission of Sc_Y and Sc_{Lu} centers in the bands at 313 and 290 nm, respectively, dominates in the luminescence of YAG:Sc and LuAG:Sc *SCF* (Fig.5, a and b, curve 1). The bands at 353 and 335 nm, related to the emission of Sc_{Al} centers in YAG and LuAG *SCF*, respectively, become dominant at larger (x=0.15-0.4 f.u.) scandium concentration (Fig.5a and 5b, curve 2) which correlate with substantial increase of the LY of these *SCF* (Fig.4, Table 1). Maximum of the LY of YAG:Sc and LuAG:Sc *SCF* is reached at x=0.3-0.4 f.u. (Fig.4). At highest Sc content the concentration quenching of Sc^{3+} related centers occurs.

The luminescence decay kinetics of the $Sc_{Y,Lu}$ and Sc_{Al} centers at 300K is shown in Fig.5c on example of LuAG:Sc *SCF*. Under excitation with energy of 6.88 eV in exciton range the main components of the Sc_{Lu} center luminescence in LuAG:Sc decay with a time of 245 ns (Fig.6, curve 1). The decay time of the dominant component of the Sc_{Al} center luminescence at 300K (Fig.5c, curve 2) is equal to 390 ns.

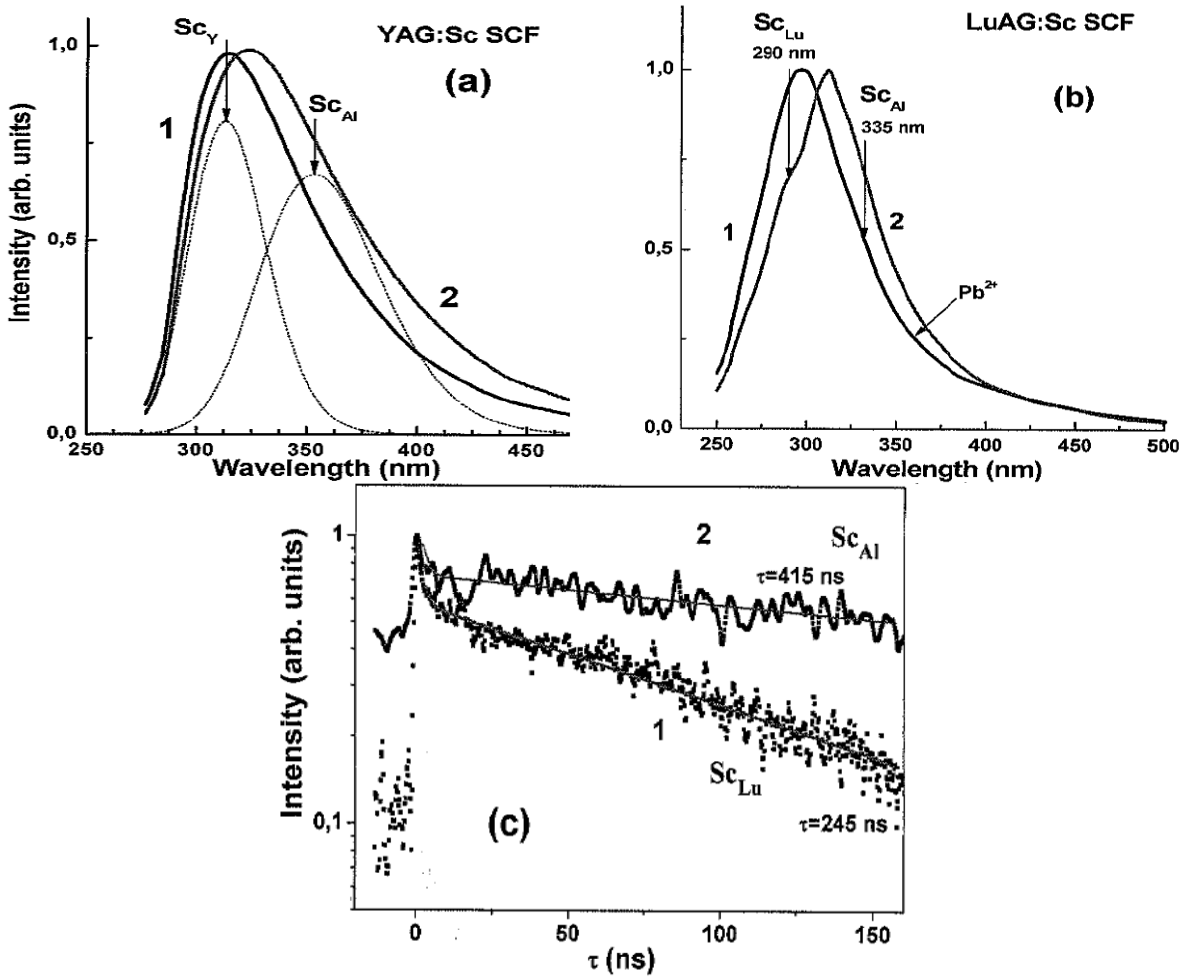

Figure 5 CL spectra of YAG:Sc (a) and LuAG:Sc (b) *SCF* with different Sc content at 300K. The content of Sc_2O_3 oxide in MS was 4.6 and 6.7 mole % (curves 1) and 10.4 and 9.8 mole % (curves 2), respectively. The decomposition of spectrum 2 in Fig.5a is given by the dashed lines. (c)-decay kinetics of the luminescence of Sc_{Lu} centers at 280 nm (1) and Sc_{Al} centers at 335 nm (2) in LuAG:Sc *SCF* under excitation by SR with an energy of 6.88 ev at 300K.

The LY of YAG:Sc and LuAG:Sc *SCF* and *SC* scintillators is strongly depend on the total Sc content and distribution of Sc^{3+} dopant over the {c}- and (a)-positions in garnet host. Specifically, the concentration of $Sc_{Y,Lu}$ and Sc_{Al} centers in YAG *SCF* can be significantly changed by substitution of the {c}- and (a)-sites of garnet lattice by Lu^{3+} and Ga^{3+} ions with smaller or larger ionic radii, respectively, than that in Y^{3+} and Al^{3+} cations. Such substitution is strongly reflected on the LY of *SCF* scintillators. Specifically, the Lu^{3+} co-doping leads to increasing the LY of YAG:Sc *SCF*, whereas the Ga^{3+} co-doping decrease of the LY of these scintillators (Table 1). As can be seen from Table 1, the LY of (YLu)AG:Sc and LuAG:Sc *SCF* scintillators at the optimal Sc^{3+} content 0.4-0.6 f.u. is comparable with their *SC* analogues and reaches values about 50% of YAP:Ce and (LuY)AP:Ce standard crystal. This result shows that influence of Pb^{2+} dopant on the UV luminescence of Sc^{3+} - based centers is not so much significant as that on the luminescence of Ce^{3+} ions in *SCF* of perovskites and the luminescence of Pr^{3+} ions in *SCF* of garnets. It is most important that this allows to use PbO-based flux for producing *SCF* scintillators with high LY emitting in UV range.

4. X-ray excited luminescence spectra of SCF

The emission spectra in 300-750 nm range of the tested LuAG:Pr/YAG, LuAG:La/YAG, LuAG:Sc/YAG and LuAP:Ce/YAP epitaxial structures with the SCF thickness of 0.8, 1.7,5.0 and 2.3 μm, respectively, under X-rays excitation in the direction perpendicular to *SCF* surface, were measured with Oriel 77233 grating (1200l/mm, blazed at 500 nm) monochromator and Hamamatsu R4632 PMT assembly. The X-rays were operated with a Cu anode (25kV, 40mA) and a 25μm copper filter for selection of the dominant 8keV line of copper for preferable excitation of *SCF* scintillators. At the same time, the partial excitation of YAG and YAP substrates by the 8 keV X-ray is also expected due to low (1.7-8 μm) thickness of *SCF*. All spectra were corrected for the grating wavelength response and the photomultiplier quantum efficiency. The results are presented in Fig.6.

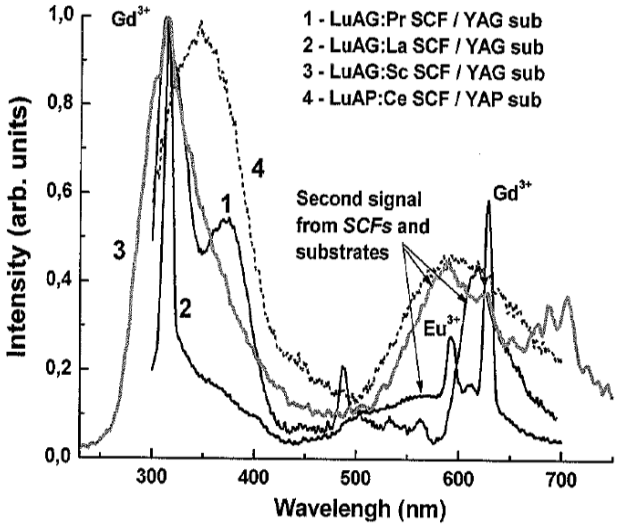

Figure 6. X-ray excited ($Cu_{K\alpha}$) luminescence spectra of LuAG:Pr/YAG (1), LuAG:La/YAG (2), LuAG:Sc/YAG (3) and LuAP:Ce/YAP (4) epitaxial structures at 300K.

The X-rays excited emission spectra of LuAG:Pr/YAG, LuAG:Sc/YAG and LuAP:Ce/YAG epitaxial structures in UV range (Fig.6, curves 2 and 3) with a *SCF* thickness of 8, 5 and 2.3 μm, respectively, are very close to the CL spectra of their *SCF* components (Fig.1,curve 1, Fig.2, curve 1 and Fig.3b, curve 2,respectively). At the same time, the X-rays excited emission spectra of LuAG:La/YAG epitaxial structure in UV range due to small (1.7 μm) *SCF* thickness present superposition of the luminescence of LuAG:La *SCF* and YAG substrate (Fig.2, curves 2 and 3, respectively). It is necessary to note that apart from the visible emission of Pr^{3+} and Pb^{2+} ions, all epitaxial structures also reemit the part of UV light in

the visible range (Fig.6, curves 1-4). Specifically, the sharp line bands peaked at 592, 610 and 627 nm in the emissions spectra of LuAG:La/YAG epitaxial structure are caused by Eu^{3+} ions emission and the second order of the UV emission of Gd^{3+} ions as trace impurities in YAG substrate. Therefore, for detection of X-ray image only in UV light, the use of a band-pass filter is strongly required, in order to cut the visible emission of scintillators.

We also estimate the conversion efficiency of the tested *SCF* scintillators into the UV and visible ranges under X-ray excitation. The conversion efficiency is measured with an imaging system equipped with microscope objective 4x and CCD camera. The X-rays from copper anode, operated at 20kV, 50mA, were additionally separated by 25μm copper filter for receiving 8keV line of copper. The *SCF* are exposed for 30 s and an average value of the intensity is taken on the final image. The image is corrected from detection system response to wavelength and *SCF* thickness (X-ray absorption). All the results are compared to the conversion efficiency of the reference YAG:Ce *SCF* scintillator. The characteristics of tested *SCF* samples under X-ray excitation are summarized in Table 2.

Table 2 Characteristics of LuAG:Sc/YAG, LuAG:La/YAG, LuAG:Pr/YAG and LuAP:Ce/YAP epitaxialstructures under excitatiom by 8keV X-ray (CuKα) excitation. Conversion efficiency of LuAG:La/YAG structure was measured without correction on the part of UV emission below 320 nm, which was cut by the objective used.

***SCF* scintillators**	**LuAG:La**	**LuAG:Sc**	**LuAG:Pr**	**LuAP:Ce**
Thickness, μm	1.7	5.0	8	2.3
Main emission lines (nm)	280, 315	313.5	315, 375	360
Conversion light yield, % with respect to YAG:Ce *SCF*	95 % (λ >320 nm)		100 % (λ>320 nm)	20 %
Afterglow @20ms (2s exposure to X-rays)	0.05 %		0.29 %	0.14 %
Afterglow @1000ms (2s exposure to X-rays)	0.001 %		0.007 %	0.07 %

5.Afterglow

The afterglow (delayed luminescence) is measured after X-rays excitation (Mo-anode) with an exposure time of 2 s (typical exposure time at ESRF is 0.1-10 s). The setup is made of a PMT2020Q and a SR400 gated photon counter (Stanford Research Instrument) working in the counting mode. The time resolution of the setup is 4 ms. The results of measurements of afterglow of LuAG:La, LuAG:Pr and LuAG:Ce *SCF* scintillators in comparison with recently developed [5,6] LuAG:Eu and YAG:Ce *SCF* are presented in Fig.7 and Table 2.

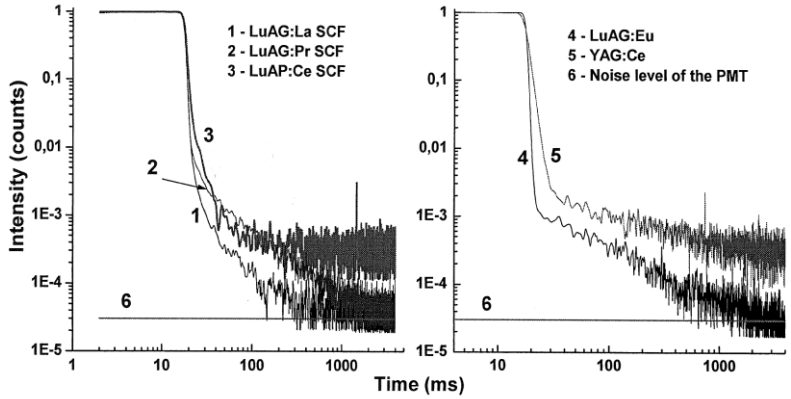

Figure 7. Afterglow of LuAG:La(1),LuAG:Pr(3) and LuAP:Ce *SCF* scintillators in comparison with recently developed [5,6]LuAG:Eu and YAG:Ce *SCF* scintillators following a 2s X-ray pulse exposition

As can be seen from Fig.7, the LuAG:La and LuAG:Pr SCF scintillators shows three decay decades in the 12 and 44 ms time intervals and four decay decades in the 30 and 100 ms time intervals, respectively (curves 1 and 2). The LuAP:Ce CF scintillators shows at least 3 decay decades in the 30 ms time interval. For comparison, recently developed [5,6] LuAG:Eu and YAG:Ce *SCF* shows three decay decades in the 5 and 55 ms time intervals, respectively (Fig.7, curve 4 and 5). At the same time, four decay decades for LuAG:Eu *SCF* was obtained in the significantly largest (384 ms) time intervals. Unfortunately, the dynamic of the measurement does not allow to obtain the temporal response from LuAP:Ce and YAG:Ce *SCF* samples behind 4 decades (see Fig.7, curve 3 and 5, respectively).

6.Visualisation of X-Ray images with UV – emitting SCF scintillators

6.1 Flat field X-rays images

Flat field images of the surface of tested LuAG:La, LuAG:Pr and LuAG:Ce *SCF* scintillators were obtained using no-filtered X-ray excitation (Cu anode operated at 25 keV, 45 mA). The Sensicam (PO) CCD camera was used as a recording device. The objective magnification was 4x. For LuAG:Pr and LuAG:La *SCF* only a part of their emission spectra contributes to the images because using the glass objective cuts the emission with the wavelength below 320 nm. The results are presented in Fig.8.

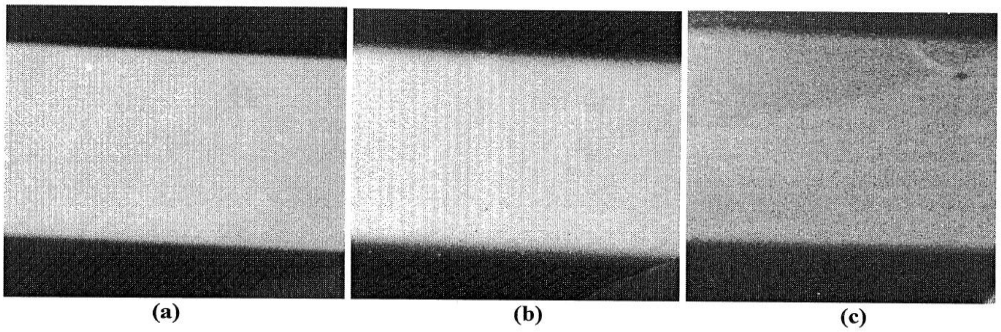

Figure 8. Flat-field image of LuAG:La (a), LuAG:Pr (b) and LuAP:Ce (c) *SCF*. Some defects on the surface of the *SCF* scintillators can be seen

6.2 Imaging in UV light

We also tested the LuAG:Pr and LuAG:La *SCF* scintillators at ESFR for visualization of image of X-ray radiated standard objects (resolution target) in the UV light. Our experimental system included the UV objective 15x, UV mirror, bandpass filter peaking at 320 nm and Sensicam QE CCE camera (from PCO). We could acquire images in the time less than 5 s with under excitation by X-ray quanta with an energy of 20 keV and a flux of $2 \cdot 10^{10}$ photons/sec both using the total emission spectrum (UV + visible) of LuAG:Pr or LuAG:La *SCF* scintillators (Fig.9a) or narrow part of the UV emission bands around 320 nm (Fig.9b).

The first image of resolution target was obtained with a spatial resolution of about 1.5 μm using only of the UV part of light of LuAG:La *SCF* scintillators (Fig.9b). The image resolution is comparable with quality of the image obtained with using total spectrum of LuAG:La and LuAG:Pr *SCF* (Fig.9a). These first results of testing are really encouraging. The UV emission of LuAG:La and LuAG:Pr *SCF* scintillators is efficient enough to be used for detection of the UV light following X-ray to UV conversion. That can be an interesting aspect for improving the resolution of high – resolution imaging detectors used in SR applications.

Nevertheless, we believe that the resolution of image in the UV light, presented in Fig.9b, can be significantly improved in future. The main problem of decreasing the resolution of the detector is connected with the large part of the UV light, emitting from the substrate, which then reemits in the visible range (Fig.6). Therefore, the ratio of the UV light coming from *SCF* and substrate must be substantially increased for the studied compounds by the way of increase of the total LY of *SCF* scintillators. We plan to test other UV-emitting *SCF* scintillators with relatively higher LY, specifically LuAG:Sc, LuYAG:Sc *SCF* (Table 1) as well as LuAG:Bi *SCF* [16] for visualization of X-ray image in the UV light. We also expect that a increase of the LY of LuAG:Pr and especially LuAP:Ce *SCF* scintillators can be achieved by means of using of **lead-free fluxes** for their crystallization by LPE method. Namely,

we obtain the first good results on YAP:Ce *SCF* crystallization from $BaO-B_2O_3-BaF_2$ flux [24] with comparable LY in comparison with the same SCF grown from the PbO-based flux with strongly exponential decay kinetic of Ce^{+3} emission (Table 1).

7. Conclusion

Development of three types of UV –emitting single crystalline film (*SCF*) scintillators grown by liquid phase epitaxy methods (LPE) is considered in this work:

1) Ce^{3+} doped *SCF* of Y-Lu-Al perovskites, where the fast and intensive f-d luminescence of Ce^{3+} ions with a decay time of 16-17 ns occurs in the 360-370 nm range;
2) Pr^{3+} doped *SCF* of Y-Lu-Al garnets, where the fast and intensive f-d luminescence of Pr^{3+} ions in the 300-400 nm range with decay time 13-17 ns is realized;
3) *SCF* of Y-Lu-Al-garnet compounds doped with La^{3+} or Sc^{3+} isoelectronic impurities emitting in the 290-400 nm range due to formation of $La_{Y,Lu}$ or $Sc_{Y,Lu}$ and Sc_{Al} emission centers with the decay time of the luminescence in several hundred ns range.

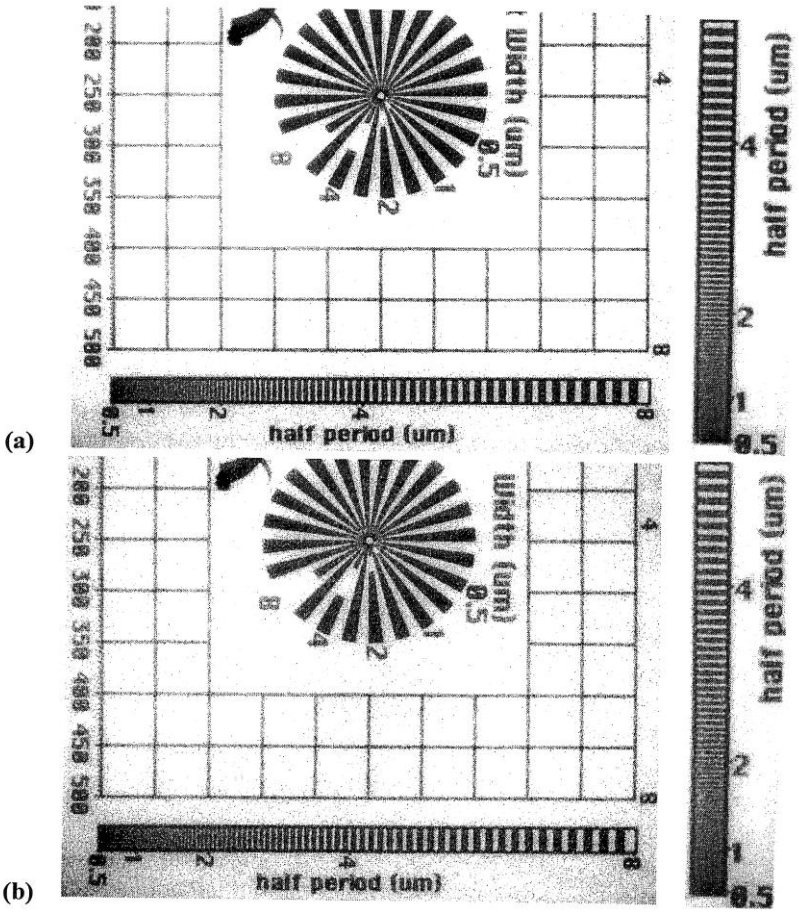

Figure 9. Images of resolution target obtained using the total spectrum (UV+visible) (a) and only of UV part of emission (b) of LuAG:La *SCF* scintillator

We have tested several novel UV-emitting LuAG:Pr, LuAG:La and LuAP:Ce SCF scintillators for visualization of X-ray images at ESFR. The UV emission of the LuAG:Sc,LuAG:La and LuAG:Pr *SCFs* is efficient enough for conversion of X-ray to UV light. This can be an interesting alternative to increase the resolution of imaging detectors used in synchrotron radiation applications. The first image with a

spatial resolution of about 1.5 μm of resolution target was obtained using only of the UV part of light of the LuAG:La *SCF* scintillators.

The main problem in the development of these types of scintillators by LPE method from the traditional $PbO\text{-}B_2O_3$ flux is connected with the significantly larger influence of Pb^{2+} flux dopant on the UV luminescence of Pr^{3+} ions in *SCF* of garnets and Ce^{3+} ions in *SCF* of perovskites than in the case of recently developed YAG:Ce and LuAG:Ce *SCF* scintillators emitting in the visible range. This is the main reason for lower (by 2-3 times) LY of Pr – doped YAG and LuAG *SCF* and significantly lower (by 4-7.6 times) LY of Ce-doped YAP and LuAP *SCF* scintillators in comparison with their single crystals analogues. At the same time, the influence of Pb^{2+} dopant on the UV luminescence of La^{3+} and especially Sc^{3+} - based centers is not so significant than on the luminescence of Ce^{3+} and Pr^{3+} ions in *SCF* of perovskites and garnets. This allows using PbO-base flux for producing *SCF* scintillators emitting in the UV range with high LY.

The possible ways for improvement of figure-of-merit of UV-emitting *SCF* scintillators are discussed. Specifically, future development of UV scintillators based on Ce^{3+} -doped *SCF* of perovskites, and Pr^{3+}, La^{3+} and Sc^{3+} doped *SCF* of garnets strongly demands the use of alternative lead-free fluxes for their crystallization. In this work, we present the set of results related to using the $BaO\text{-}B_2O_3\text{-}BaF_2$ flux for crystallization of UV –emitting YAP:Ce *SCF* perovskites. We show, that the advantageous properties of YAP:Ce *SCF* scintillators, grown from the BaO – based flux, with respect to those grown from the traditional PbO – based flux, are connected with removing the additional channels of dissipation of excitation energy on the luminescence and trapping charge carriers at Pb – based centers.

Acknowledgement
This research was supported by Czech Science Foundation (project no. 202/08/0893) and Ministry of Education and Science of Ukraine (projects No DZ/296-2008 and no SL-28F).

References

[1] Robertson J M, van Tol M V 1984 Cathodoluminescent garnet layers *Thin Solid Films* **114**(1-2) 220-40
[2] Zorenko Yu V, Novosad S S, Pashkovskii M V, Lyskovich A B, Savitskii V G, Batenchuk M M, Malyutenkov P S, Patsagan N I, Nazar I V and Gorbenko V I 1990 Epitaxial structures of garnets as scintillators detectors of ionizing radiation *Journal of Applied Spectroscopy* **52**(6) 645-49
[3] Ferrand B, Chambaz M and Couchaud M 1999 Liquide phase epitaxy. A versalite technique for the development of miniature optical components in single crystal dielectric media. *Optical Materials* **11** 101-14
[4] Globus M, Grinyov B, Ratner M, Tarasov V, Lyubinskiy V, Vyadi Y, Ananenko A, Zorenko Y, Gorbenko V and Konstankevych I 2004 New type of scintillation detectors for biological , medical and radiation monitoring applications. *IEEE Transact. on Nucl.Sci*. **51**(3) 1297-303
[5] Koch A, Raven C,Spanne P and Snigirev A 1998 X-ray imaging with sub-micrometer resolution employing transparent luminescent screens. *J.Opt.Soc.Am.* **A** 15 1940-51
[6] Koch A, Peyrin F, Heurtier P, Chambaz B, Ferrand B, Ludwig W and Couchaud M 1999 An X –ray camera for computed microtomography of biological samples with micrometer resolution using $Lu_3Al_5O_{12}$ and $Y_3Al_3O_{12}$ scintilators 1999 *Proc.SPIE* **3659** 170-9
[7] Martin T and Koch A 2006 Recent development in X-ray imaging with micrometer spatial resolution *Journal of Synchrotron Radiation* **13** 180-94
[8] Zorenko Yu, Batenchuk M, Pashkovsky M, Konstankevych I, Gorbenko V, Yurchushyn P, Martynova V and Duzyj T 1998 Single crystalline film sensors for cathode-ray tubes: possibilities of application, peculiarities and light parameters, *Proc.SPIE* **3359** 261-64
[9] Hrytskiv Z D, Zorenko Y, Gorbenko V,Peden A D and Shkliarskyi V I 2007 Single crystalline film screens for cathode-ray tubes: New life of television scanning optical microscopy. *Radiation Measurements* **42** (4-5) 933-36

[10] Zorenko Yu V, Konstankevich I V, Gorbenko V I and Yurchishin P I 2002 *Journal of Applied Spectroscopy* **69** 769-76
[11] Zorenko Yu, Gorbenko V, Konstankevich I, Grinev B and Globus M 2002 Scintillation properties of $Lu_3Al_5O_{12}$:Ce single crystalline films *NIM* A**486** 309-14
[12] Zorenko Yu, Gorbenko V, Konstankevych I, Voloshinovskii A, Stryganyuk G, Mikhailin V, Kolobanov V and Spassky D 2005 Single – crystalline films of Ce-doped YAG and LuAG phosphors: advantages over bulk crystals analogues *Journal of Luminescence* **114** (4) 85-94
[13] Zorenko Y, Gorbenko V,Mihokova E, Nikl M,Nejezchled K,Vedda A,Kolobanov V and Spassky D Single crystalline film sicintilators based on Ce-and Pr-doped aluminium garnets 2007 *Radiation Measurements* **42** 521-27
[14] Nikl M, Mihokova E, Pejchal J, Vedda A, Zorenko Yu and Nejezchled K 2005 The antisite Lu_{Al} defect – related trap in $Lu_3Al_5O_{12}$:Ce single crystal *Phys.Stat.Sol*. b **242** R119-21
[15] Prsusa P,Cechak T,Mares J A, Nikl M, Zorenko Yu V, Gorbenko V I, Tous J and Blazek K 2008 The α-particle excited scintillation response of the liquid phase epitaxy grown LuAG:Ce thin films *Applied Physics Letters* **2**(1) 1-3
[16] Zorenko Yu, Voloshinovskii A,Savchyn V, Vozniak T,Nikl M, Nejezchled K, Mikhailin V, Kolobanov V and Spassky D 2007 Exciton and antisite defect – related luminescence in $Lu_3Al_5O_{12}$ and $Y_3Al_5O_{12}$ garnets *Phys.Stat. Sol*. b **244** 2180-89
[17] Nikl M, Pejchal J, Yoshikawa A, Fukuda T, Krasnikov A, Vedda A, and Nejezchleb K 2006 Pr^{3+} doped novel single crystal scintillators ed.Getkin A and Grinyov B *SCINT 2005 Proc.of the 8 Inter.Conf. on inorganic scintillators and their use in science and industrial applications*, Alishta, Crimea Ukraine, Kharkiv 89-94
[18] Zorenko Y and Gorbenko V 2007 Growth peculiarities of the $R_3Al_5O_{12}$ (R=Lu,Yb,Tb,Eu-Y) single crystalline film phosphors by Liquid Phase Epitaxy *Radiation Measurements* **42** 907-10
[19] Zorenko Y, Gorbenko V, Konstankevych I, Voznjak T, Savchyn V, Nikl M, Mares J A, Nejezchleb K, Mikhailin V, Kolobanov V and Spassky D 2007 Peculiarities of luminescence and scintillation properties of YAP:Ce and LuPA:Ce single crystals and single crystalline films *Radiation Measurements* **42** 528-32
[20] Zorenko Y, Gorbenko V, Batentschuk M and Winnacker A 2009 Growth and luminescent properties of single crystalline films of $RAlO_3$ (R=Lu,Lu-Y,Y,Tb) perovskites *Phys.Stat.Sol.* accepted
[21] Zorenko Yu, Konstankevych I, Gorbenko V and Zorenko T 2002 Growth and characteristics of crystallophosphors on the base of single crystalline films of LuAG and YAG garnets 2002 *Molecular Physics Reports* **36** 127-32
[22] Zorenko Yu, Gorbenko V and Konstankevych I 2003 Peculiarities of growth of phosphors based on the single crystalline films of garnets by liquid phase epitaxy method *Surface* **5** C83-90
[23] Babin V,Gorbenko V,Makhov A,Mares J A, Nikl M, Zazubovich S and Zorenko Yu 2007 Luminescence characteristics of $Pb^{2}+\rightarrow Ce^{3+}$ energy transfer processes *Journal of Luminescence* **127**(2) 384-90
[24] Zorenko Y, Gorbenko V, Savchyn V, VoznyakT, Nikl M, Mares J A, Beitlerova A and Kucerkova R 2009 The luminescent and scintillation properties of YAP and YAP:Ce single crystalline films grown by liquid phase epitaxy from BaO-based flux *Phys.Stat.Sol.* a submitted;
Globus M and Grinyov B 2000 *Non – inorganic scintillators* (Akta, Kharkiv)
[25] Babin V, Bichevin V, Gorbenko V, Makhov A,Mhokova E,Nikl M, Vedda A, Zuzubovich S and Zorenko Yu 2009 Luminescence of dimmer lead centers in aluminium perovskites and garnets *Phys.Stat.Sol*. B **246**(6) 1318-26
[26] Gorbenko V,Krasnikov A, Nikl M, Zuzubovich S and Zorenko Yu 2009 Luminescence characteristics of LuAG:Pr and YAG:Pr crystalline films *Optical Materials* **31** 1805-07
[27] Valbis J A, Volzhenskaja L G,Dubov Yu G, Zorenko Yu V, Nazar I V and Patszagan N I 1987 Luminescence centers in single crystalline compounds of yttrium-aluminium garnet doped by scandium isoelectronic impurity *Optics and Spectroscopy* **63** 1058-63

[28] Zorenko Yu V 2006 Luminescence of La^{3+} and Sc^{3+} isoelectronic impurities in $Lu_3Al_5O_{12}$ single crystalline films *Optics and Spectroscopy* **100** 572-80
[29] Zorenko Y, Mares J A, Kucerkova R, Gorbenko V, Savchyn V,Voznyak T, Nikl M,Beitlerova A and Jurek K 2009 Optical, luminescence and scintillation characteristics of the Bi-doped LuAG and YAG single crystalline films *J.Phys*.D *Appl Phys*. **42** 7